

doi: 10.3788/gzxb20144306.0625001

强光照射下的 InGaAs 二极管内部光生载流子分析

胡伟, 豆贤安, 孙晓泉

(脉冲功率激光技术国家重点实验室, 电子工程学院, 合肥 230037)

摘 要: 以 InGaAs p-i-n 管为例, 研究了光电二极管在激光脉冲作用下非线性响应的内部机理特征, 计算分析了二极管在强光辐照下内部空间电荷屏蔽效应对器件光电响应特性产生的影响. 通过计算耗尽区的电场强度、载流子分布和电子-空穴的漂移速度, 发现低偏置电压或强光辐照都会使耗尽区的电场强度下降, 载流子的漂移和扩散速度降低到非饱和状态, 使光生载流子的复合率下降, 大量载流子聚集在耗尽区内, 形成了空间电荷屏蔽效应, 导致二极管呈非线性响应状态. 在 5 V 偏置电压条件下, 增加皮秒激光的脉冲能量, 光电二极管的光伏电压响应脉宽逐渐展宽, 峰值电压呈非线性变化.

关键词: 光电二极管; 非线性响应; 强光辐照; 空间电荷屏蔽; 耗尽区

中图分类号: TN364

文献标识码: A

文章编号: 1004-4213(2014)06-0625001-5

The Analysis of the Photo-carriers of the InGaAs p-i-n Photodiode Response to the High Optical Injection

HU Wei, DOU Xian-an, SUN Xiao-quan

(State Key Laboratory of Pulsed Power Laser Technology, Electronic Engineering Institute, Hefei 230037, China)

Abstract: To study the internal mechanism of the photodiode nonlinear response to the high energy laser pulse, the influence of the space charge screening on the photoelectric response characteristic of the InGaAs p-i-n photodiode was calculated under the high optical injection. The electrical field, distribution of carriers and electron-hole mobility in the depletion region were calculated respectively. The simulated results indicate that when the applied bias field is low or the laser pulse energy is high, the electrical field in the depletion region is suppressed and the drift-diffusion velocity is reduced to the unsaturated state. Therefore, the separation and recombination of the hole-electron is slowed down, lots of the photo-carriers is in the depletion region, which leads to the nonlinear response due to the space charge screening. In the experiment, the InGaAs p-i-n photodiode's response voltage pulse width is widening and the peak voltage is increasing nonlinearly with the increasing 20 ps laser pulse energy in the 5 V applied bias. The calculation of the photodiode internal mechanism is proved to be valid by the experimental phenomena.

Key words: Photodiode; Nonlinear response; High optical injection; Space charge screening; Depletion region

OCIS Codes: 250.0040; 230.0230; 230.4320; 230.0040; 230.0250

Foundation item: The Key Laboratory Foundation (No. 13J1003)

First author: HU Wei(1986-), male, Doctoral candidate, mainly focuses on optoelectronic technology. Email: double8844@163.com

Supervisor(Contact author): SUN Xiao-quan(1962-), male, professor, Ph. D. degree, mainly focuses on optoelectronic technology. Email: sunxq@ustc.edu

Received: Oct. 22, 2013; **Accepted:** Dec. 29, 2013

<http://www.photon.ac.cn>

0 Introduction

With the rapid development of the modern optical communication, the high requirements of the optical receiving terminal are proposed such as the higher saturated power and output current^[1-4]. High-current InGaAs-InP photodiode is a key and suitable component for the optical communication system because it could increase the receiver dynamic range and the signal to noise ratio in the modulated links^[5]. However, to obtain the high output current, the photodiodes would be saturated due to the increased optical injection. Because of the nonlinearity, the photodiode's responsivity reduces and the output saturated current decreases^[6]. Therefore, the mechanism and effect of the nonlinearity should be studied further to improve the photodiode's saturated output by designing of the suitable optical device.

The primary influence on the photodiodes due to the nonlinearity is the electric field screening induced by the high photo-generated carriers. Since the nonlinear response was found in 1980s, it have attracted lots of attention from the researchers, including absorption saturation nonlinearity^[6], heating effect^[7], trapping recombination^[5] etc. Although the work for analyzing the screening effect is conducted by computing some simultaneous equations^[8] or doing some careful experiments^[9], the internal mechanism and status of the carriers due to the space charge screening effect in the photodiode should be analyzed further, such as the electrical field distribution, the carrier distribution, the mobility and so on.

In this paper, to study the space charge screening effect in-depth, the photo-generated carriers in the depletion region of the InGaAs p-i-n photodiode were analyzed and discussed based on the drift-diffusion mechanism. The carriers distribution and the space electric field were calculated. At last, the characteristic of the InGaAs p-i-n photodiode response signal to high optical injection was confirmed by the experiment.

1 Mathematical model

1.1 The simulation device

The device is a p-side illuminated InGaAs photodiode with a 354 μm thickness and 1 mm diameter, whose cylindrical symmetry structure is shown in Fig. 1. Photons enter the photodiode by passing through the p-InP cap (thickness is 1 μm and the doping concentration is 10^{18} cm^{-3}) into the n-InGaAs (thickness is 2 μm and the doping concentration is 10^{15} cm^{-3}) depletion region. The InP is selected to cap layer due to its wide bandgap to restrain the absorption

in the p region by the heterojunction's window effect which could improve the detector's quantum efficiency and response speed.

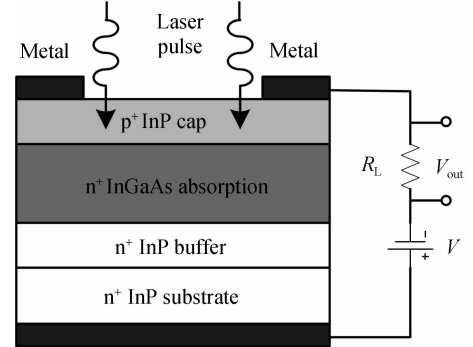


Fig. 1 InP/InGaAs photodiode cylindrical structure

1.2 Basic simulation equation

The calculation is performed within the thermodynamic drift-diffusion framework by simultaneously solving the Poisson and electron-hole continuity equations^[8].

$$\nabla \cdot \epsilon_r \epsilon_0 \nabla \varphi = -q(p - n + N_D^+ - N_A^-) - \rho_s \quad (1)$$

$$\begin{cases} \frac{\partial n}{\partial t} = \frac{1}{q} \nabla \cdot \mathbf{J}_n - (U_n - G_n) \\ \frac{\partial p}{\partial t} = -\frac{1}{q} \nabla \cdot \mathbf{J}_p - (U_p - G_p) \\ \mathbf{J}_n = q\mu_n n \mathbf{E}_n + qD_n \nabla n \\ \mathbf{J}_p = -q\mu_p p \mathbf{E}_n - qD_p \nabla p \end{cases} \quad (2)$$

$G_{n,p}$ is the electron or hole generation rate, $U_{n,p}$ is the net electron or hole spontaneous recombination rate, \mathbf{J}_n and \mathbf{J}_p are electron and hole current flux density respectively, which is the sum of drift and diffusion currents density. D_n and D_p are diffusion coefficients of the electron and hole respectively. They meet with the Einstein relation $\frac{D_n}{\mu_n} = \frac{D_p}{\mu_p} = \frac{kT}{q}$.

When the carriers recombination rate is calculated in the InGaAs photodiode, the Shockley-Read-Hall, Auger and direct recombination are considered

$$U_{\text{SRH}} = \frac{pn - n_{ie}^2}{\tau_p \left[n + n_{ie} \exp\left(\frac{E_{\text{trap}}}{kT}\right) \right] + \tau_n \left[p + n_{ie} \exp\left(\frac{-E_{\text{trap}}}{kT}\right) \right]} \quad (3)$$

$$U_{\text{auger}} = \left(nC_{n0} \left(\frac{T}{300}\right)^{\alpha_{\text{aug},n}} + pC_{p0} \left(\frac{T}{300}\right)^{\alpha_{\text{aug},p}} \right) (pn - n_{ie}^2) \quad (4)$$

$$U_{\text{dir}} = C_{\text{dir}} (np - n_{ie}^2) \quad (5)$$

here, n_{ie} is the intrinsic concentration, E_{trap} represents the difference between the trap energy level and the intrinsic Fermi energy, C_{n0} , C_{p0} and $\alpha_{\text{aug},n}$, $\alpha_{\text{aug},p}$ are the Auger coefficient and the exponent of temperature for the electrons and holes, C_{dir} is the direct recombination coefficient, τ_n and τ_p are the electron and hole lifetimes, which is relative to the concentration^[10] as shown following

$$\begin{cases} \tau_n(x, y) = \frac{\tau_{n0}}{1 + N_{\text{total}}(x, y)/N_{\text{SRH},n}} \\ \tau_p(x, y) = \frac{\tau_{p0}}{1 + N_{\text{total}}(x, y)/N_{\text{SRH},p}} \end{cases} \quad (6)$$

$N_{\text{SRH},n}$ and $N_{\text{SRH},p}$ are the Shockley-Read-Hall concentration parameters for electrons and holes. τ_{n0} and τ_{p0} are the Shockley-Read-Hall electron and hole lifetime.

The Boundary condition is determined as ohmic contacts and simple Dirichlet boundary conditions, where the surface potential φ_s and electron and hole concentrations are fixed. The surface potential is fixed at a value consistent with zero space charge,

$$\begin{cases} n + N_A^- = p + N_D^+ \\ \varphi_s = \varphi_n + \frac{kT}{q} \ln\left(\frac{n}{n_{ie}}\right) = \varphi_p - \frac{kT}{q} \ln\left(\frac{p}{n_{ie}}\right) \end{cases} \quad (7)$$

the potential φ_n and φ_p in the homogenous region are solved by the equation(1).

The carrier mobilities μ_n and μ_p are the important parameters to describe carrier transport inside the detector. In order to simulate the carrier transport more accurately when the InGaAs p-i-n photodiode is illuminated by low power laser pulse, the mobility model should contain carrier scattering effect and space charge screen effect of the high concentration carrier which are instantaneously excited by the laser pulse^[11]. With the laser power increasing, the high-injection photo-carriers further reduce the remaining electrical field and influence the velocity of the electrons and holes. In this paper, the transferred electron effect model commonly used which is the field-dependent high carriers mobility model^[5] is chose as below

$$\begin{cases} \mu_n = \frac{\mu_{s,n} + \frac{\nu_n^{\text{sat}}}{E_{//,n}} \left(\frac{E_{//,n}}{E_{0n}}\right)^4}{1 + \left(\frac{E_{//,n}}{E_{0n}}\right)^4} \\ \mu_p = \frac{\mu_{s,p} + \frac{\nu_p^{\text{sat}}}{E_{//,p}} \left(\frac{E_{//,p}}{E_{0p}}\right)^4}{1 + \left(\frac{E_{//,p}}{E_{0p}}\right)^4} \end{cases} \quad (8)$$

where E_{0n} and E_{0p} is the critical field which is set to 4kV/cm. $E_{//,n}$ and $E_{//,p}$ are the parallel electric and hole field. $\mu_{s,n}$ and $\mu_{s,p}$ are the electric and hole mobility for the surface scattering which are set to 8 000 cm²/Vs and 300 cm²/Vs^[12]. ν_n^{sat} and ν_p^{sat} are the saturated electron and hole velocity which are respectively set to 7.7×10^7 cm²/s and 4.8×10^6 cm²/s^[8]. Fig. 2 presents the velocity-field relation calculated from the previous Eq. (8).

The Fig. 2 shows that the electron-hole velocity depends on the electrical field when this field is lower than about 10kV/cm. When the electrical field is higher than 10kV/cm, the carriers velocity is tend to be steady and saturated. Therefore, the carriers

recombination depended on the difference of the electron-hole velocity is stabilized and maximized, the photodiode's responsivity is high. When the electrical field is lower than 10kV/cm, the difference between the electron-hole velocities is so significant that the holes move much slower and the response characteristic of the photodiode becomes nonlinear.

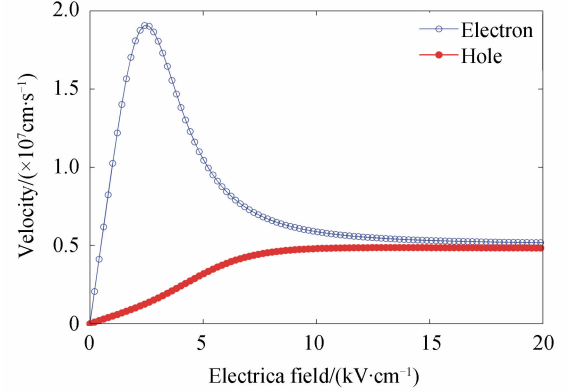


Fig. 2 Comparison of the electron and hole velocity

2 Results and analysis

2.1 Simulation

The internal electrical field of the InGaAs-InP p-i-n photodiode is calculated with different reverse bias when no light is injected as shown in Fig. 3(a). When the reverse bias is 0 V, the field in the depletion region is lower than 10 kV/cm and the carriers' drift speed is

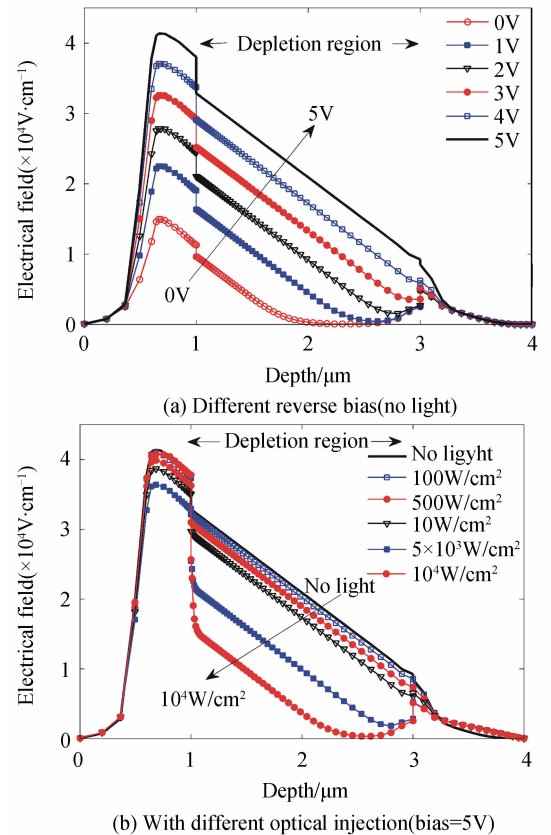


Fig. 3 Internal electrical field distribution

very low. With the reverse bias increasing, the n-InGaAs region is gradually depleted. The carriers achieve high saturate drift speed when the field in the depletion region is higher than 10 kV/cm with the reverse bias increased to 5 V, which is suitable for diffusion and drift of the photo-generated carriers.

Fig. 3 (b) shows the electrical field distribution under different optical injection with the reverse bias 5 V. With the light power increasing, the electrical field in the depletion region decreases. When the power density is $5 \times 10^3 \text{ W/cm}^2$, the field decreases to 10 kV/cm. The photo-carriers are in the unsaturated state and the recombination is decreasing. More and more photo-generated electrons and holes are in the depletion region leading to a new electrical field to suppress the applied bias field and induce a decrease of the mobility of the carriers, which is the space charge screening.

As the shown in the Fig. 4, when the photodiode is illuminated on the low power laser, the electron and hole concentration is stable at 10^{10} cm^{-3} and 10^5 cm^{-3} respectively. When the optical injection is achieved the saturate power density ($5 \times 10^3 \text{ W/cm}^2$), the electron and hole concentration is increasing to the 10^{15} cm^{-3} dramatically because of the internal electrical field decreasing due to the space charge screening.

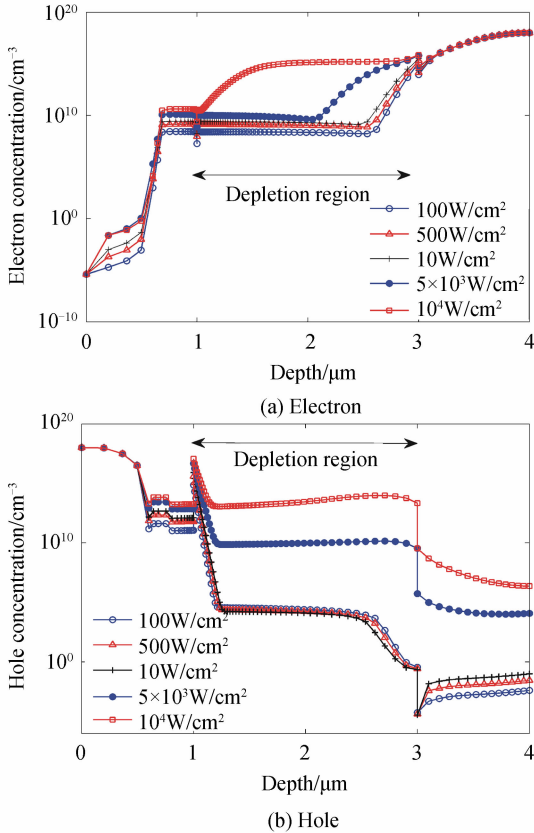


Fig. 4 Carriers distribution in the photodiode

2.2 Experiment

To affirm the simulation results, the experiment

was designed and carried out. The optical pulse wavelength, pulse duration, pulse repetition and the energy are initially set at $1.064 \mu\text{m}$, 20 ps, 20 MHz. The response signal with different the pulse energy (0.02, 0.12, 0.31, 0.54, 0.71, 0.93, 1.9 nJ) with reverse bias 5 V are shown in the Fig. 5. With the pulse energy increasing, the response voltage signal's response time begins to be longer due to the space charge screening.

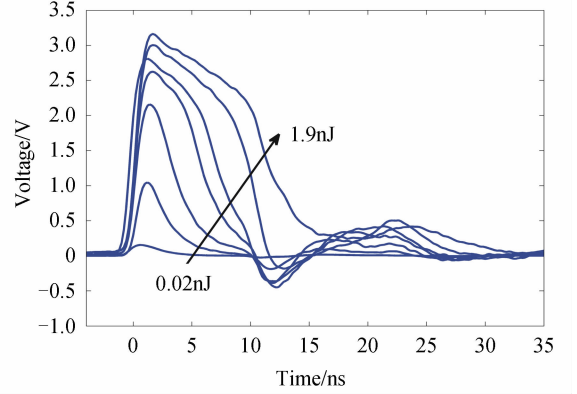


Fig. 5 Measured response signal with different pulse energy

The relationship between peak voltage and pulse energy with different reverse bias is shown in the Fig. 6. When the optical injection is low, the output peak voltage increases linearly. With the pulse energy increasing, the detector under bias 1 V is first saturation. As the reverse bias increases, the maximum linear output peak voltage and the saturated output peak voltage increase. The relationship between the peak voltage and the reverse bias under different illumination is shown in Fig. 7. With the bias increasing under a certain illumination, the detector's output peak voltage is from saturation to linearity and tending towards stability. With the increasing optical injection, the threshold of the reverse bias in the linear working region increases.

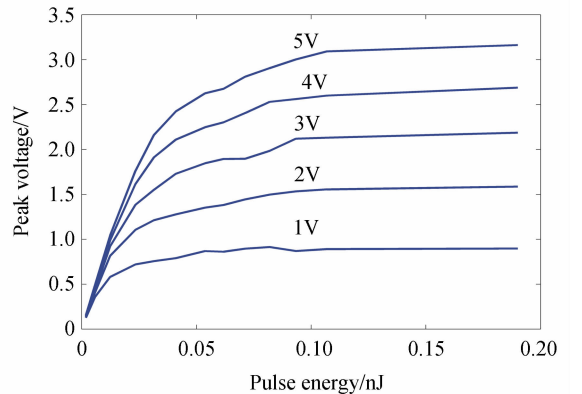


Fig. 6 Measured peak voltage dependence on the optical injection under different reverse bias

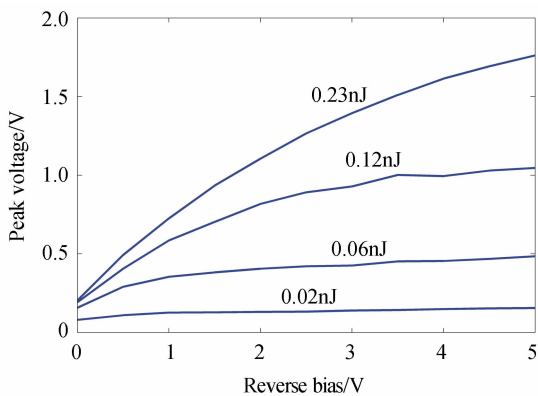


Fig. 7 Measured peak voltage dependence on the reverse bias under different optical injection

3 Conclusion

Photos enter the photodiode and be absorbed to become the photo-generated carriers. The carriers separate and recombine under the electrical field. When the optical energy is high enough to suppress the applied bias field, the difference between the electron and hole mobility became larger, lots of the slow carriers(holes) will gather in the depletion region until the photodiode exhibits nonlinear characteristics. In this paper, the nonlinearity is simulated using some proper physical models. The analysis of the mechanism is proved to be validity by the experimental phenomenon. The work in the paper could provide a theoretical basis for the design of the high output current photodiodes.

Reference

- [1] ZHANG W, LI T, LOURS M, *et al.* Amplitude to phase conversion of InGaAs pin photo-diodes for femtosecond lasers microwave signal generation[J]. *Applied physics B*, 2012, **106**(2): 301-308.
- [2] TAYLOR J, DATTA S, HATI A, *et al.* Characterization of power-to-phase conversion in high-speed p-i-n photodiodes[J]. *IEEE Photonics Journal*, 2011, **3**(1): 140-151.
- [3] ZHANG Ling-zi, ZUO Yu-hua, CAO Quan, *et al.* High-speed and high-power uni-traveling-carrier photodetector[J]. *Acta Physica Sinica*, 2012, **61**(13): 138501.
- [4] ZHU Bin, HAN Qin, YANG Xiao-Hong. High-power property of resonant-cavity-enhanced photodetectors grown on GaAs[J]. *Acta Photonica Sinica*, 2009, **38**(5): 1074-1079.
- [5] LARID J S, ONODA S, HIRAO T, *et al.* Simulation of impulse response degradation from irradiation induced trapping and recombination regions in an InGaAs on InP photodetector [J]. *Journal of Applied Physics*, 2008, **104**(8): 01-10.
- [6] JOUDAWLKIS P W, DONNELL F J, HARGREAVES J J, *et al.* Absorption saturation nonlinearity in InGaAs/InP p-i-n photodiodes[C]. in the 15th Annual Meeting of the IEEE Laser and Electro-Optics Society Glasgow, (Scotland, UK, 2002): 426-427.
- [7] DUAN N, WANG X, NING L, *et al.* Thermal analysis of high-power InGaAs-InP photodiodes[J]. *IEEE Journal of Quantum Electronics*, 2006, **42**(11): 1255-1258.
- [8] DENTAN M, DECREMOUX B. Numerical simulation of the nonlinear response of a p-i-n photodiode under high illumination[J]. *IEEE Journal of Lightwave Technology*, 1990, **8**(8): 1137-1144.
- [9] KUHLE D, HIERONYMI, BOTTCHE E H, *et al.* Influence of space charge on the impulse response of InGaAs metal-semiconductor-metal photodetectors [J]. *Journal of Lightwave Technology*, 1992, **10**(6): 753-759.
- [10] ROULSTON D J, ARORA N D, CHAMBERLAIN S G. Modeling and measurement of minority-carrier lifetime versus doping in diffused layers of n⁺-p silicon diodes[J]. *IEEE Transaction on Electron Devices*, 1982, **29**(2): 284-291.
- [11] LAIRD J S, HIRAO T, ONODA S, *et al.* High-injection carrier dynamics generated by MeV heavy ions impacting high-speed photodetectors[J]. *Journal of Applied Physics*, 2005, **98**(1): 013530.
- [12] WILLIAMS K J, ESMAN R D, DAGENAIS M. Nonlinearities in p-i-n microwave photodetectors[J]. *IEEE Photonics Technology*, 1996, **14**(1): 84-96.